

ARTICLE

**Supporting Information**

**Melamine Functionalised Multiwalled Carbon Nanotubes (M-MWCNTs) as metal-free Electrocatalyst for Simultaneous Determination of 4-Nitrophenol and Nitrofurantoin.**

Raviraj P. Dighole<sup>a,b</sup>, Ajay V. Munde<sup>a,c</sup>, Balaji B. Mulik<sup>a</sup>, Sanjio S. Zade<sup>c</sup> and Bhaskar R. Sathe<sup>a\*</sup>

a- Department of Chemistry, Dr. Babasaheb Ambedkar Marathwada University, Aurangabad-431 004 (MS) India.

b- Arts, Science & Commerce College, Badnapur 431202.

c- Department of Chemical Sciences and Centre for Advanced Functional Materials, Indian Institute of Science Education and Research (IISER) Kolkata, Mohanpur, Nadia 741246, West Bengal, India.

\*Corresponding author:

Dr. Bhaskar R. Sathe; Email: [bhaskarsathe@gmail.com](mailto:bhaskarsathe@gmail.com); [bsathe.chemistry@bamu.ac.in](mailto:bsathe.chemistry@bamu.ac.in)

Professor Sanjio S. Zade; Email: [sanjiozade@iiserkol.ac.in](mailto:sanjiozade@iiserkol.ac.in).

**List of supporting information**

**S-1) Characterisation detail**

**S-2) linear fitting plots of nitrophenol (4-NP)**

**S-3) linear fitting plots of Nitrofurantoin (NFT)**

**S-4) Effect of H<sub>2</sub>SO<sub>4</sub> on 4NP and NFT**

**S-5) Stability test of 4NP and NFT**

**S-6) Electrochemical Studies**

**Table S-1**

**Table S-2**

**S-1. Characterisation detail**

The product was analyzed via. Fourier transform infrared spectroscopy (FTIR). Its phase and structure were characterized using X-ray diffraction (XRD, Siemens D-5005 diffract meter) equipped with an X-ray tube (Cu K $\alpha$ ;  $1\frac{1}{4}$  1.5418 nm, 40 kV, 30mA, Raman spectroscopy was performed using a microscope with Raman optics (Seki Technetronic Corporation, Tokyo) with a 532 nm LASER. For EDAX analysis, the samples were prepared on Au films. X-ray photoelectron spectroscopy (XPS) on a SPECS HSA-3500 with a monochromatic Al K $\alpha$  X-ray Radiation X-ray source and hemispherical analyser was used to investigate the elemental states of the sample. Quantachrom Instruments- All electrochemical studies to perform on connected to CHI 660C electrochemical work station CHI Instrument660E, (USA) with three electrodes System. A glassy carbon electrode (GC, 3 mm dia.) was used as the working electrode to support the catalysts. A piece of Pt foil and SCE in 0.5M H<sub>2</sub>SO<sub>4</sub> were used as the counter and reference electrodes respectively.

### S-2. Linear fitting plots of Nitrophenol (4-NP)

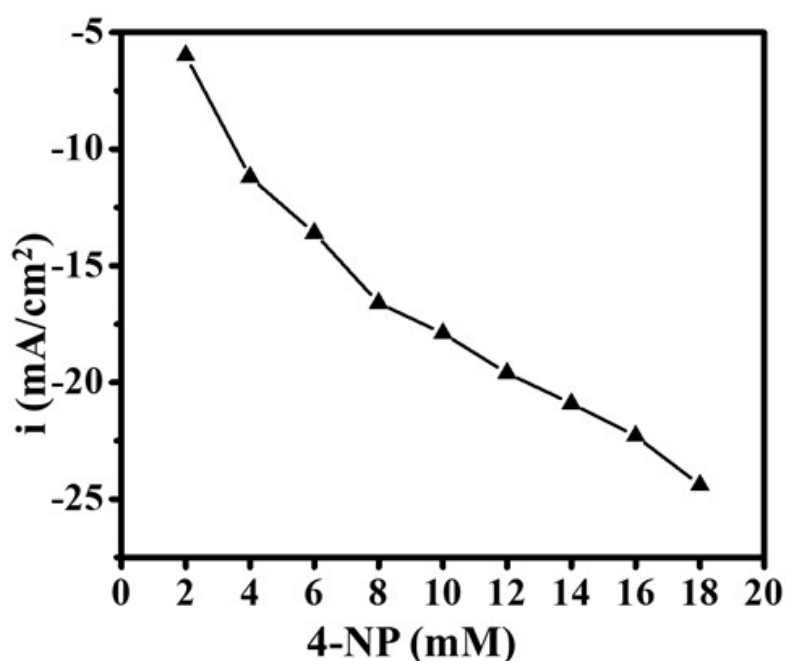


**Figure S1.** Depicts the liner fit plot for the concentration of 4-NP vs. peak current density.

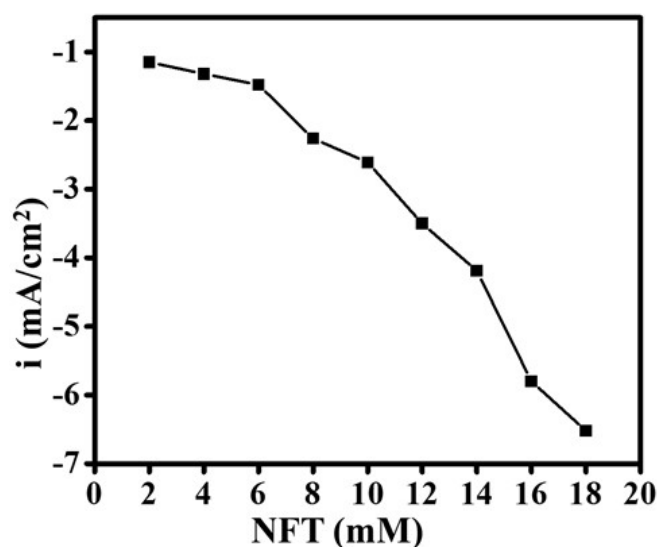
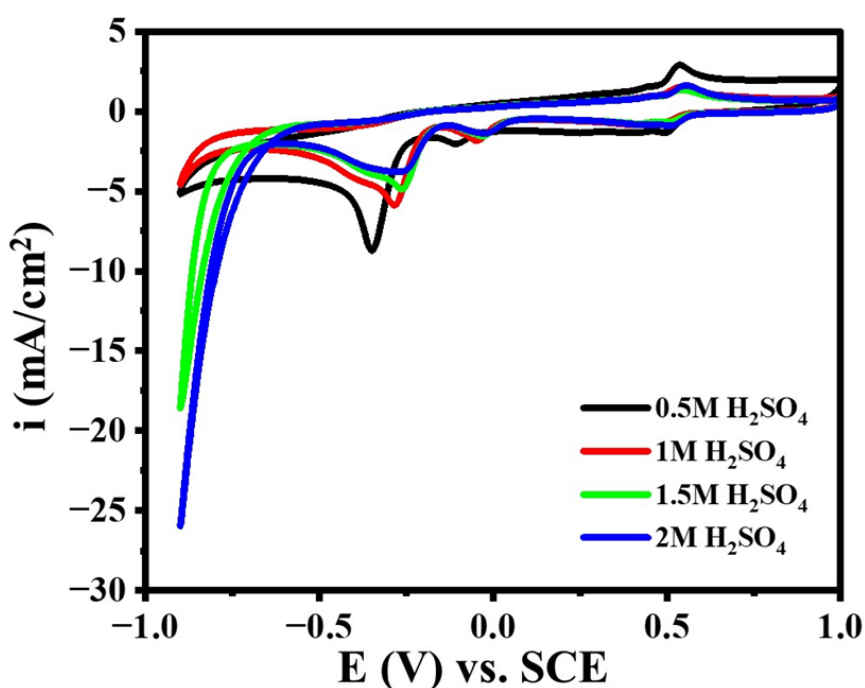
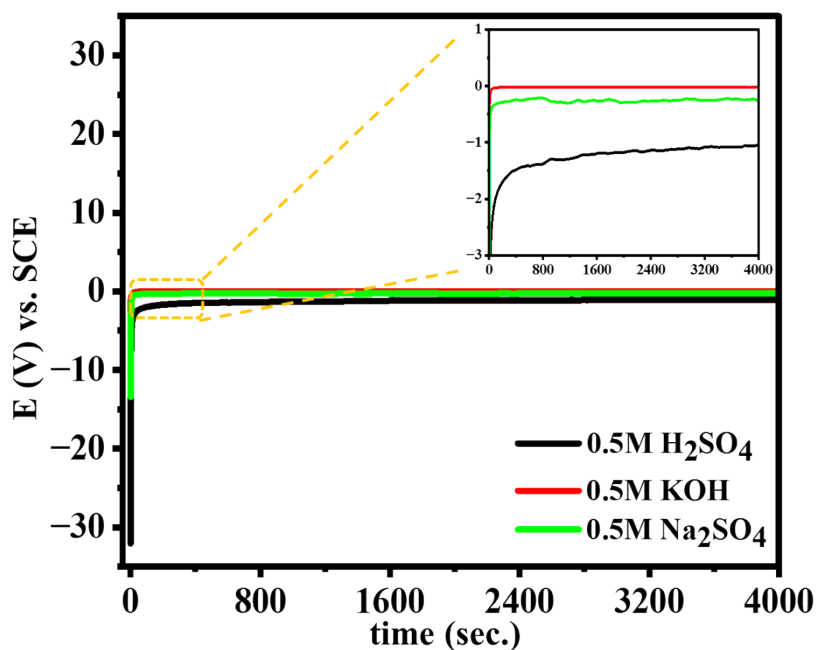
**S-3. Linear fitting plots of Nitrofurantoin (NFT):**

Figure S2. Depicts the liner fit plot for the concentration of NFT vs. peak current density.

**S-4) Effect of H<sub>2</sub>SO<sub>4</sub> on 4NP and NFT:**

**Figure S3.** Effect of Electrolyte concentration on electroreduction of 4-NP and NFT in 0.5M, 1M, 1.5M and 2M respectively at M-MWCNTs at scan rate of 50 mV/s.

**S-5) Stability test of 4NP and NFT**



**Figure S4.**  $i$ - $t$  stability tests in acidic, basic and neutral medium for 4mM 4-NP and NFT respectively vs SCE for 4000s.

#### S-6) Electrochemical Studies:

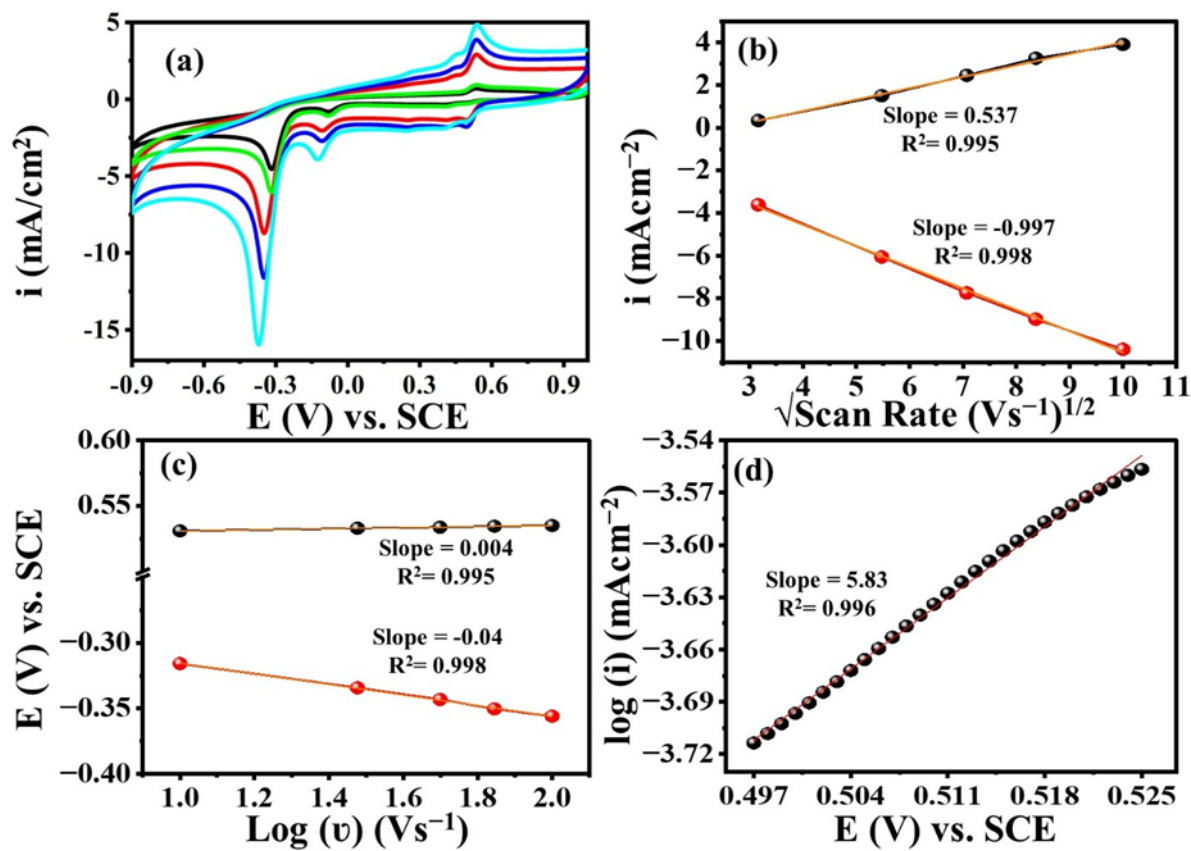


**Figure S5.** (a) Cyclic voltammograms of M-MWCNT in 0.5M H<sub>2</sub>SO<sub>4</sub> with 4mM drug + 4mM 4-NP, at different scan rates: (a) 10, (b) 30, (c) 50, (d) 70, and (f) 100 mVs<sup>-1</sup>; (b) Anodic and cathodic peak currents (*I*<sub>pa/c</sub>) versus square root of the scan rate ( $\nu^{1/2}$ ) recorded in 0.5M H<sub>2</sub>SO<sub>4</sub> with 4mM drug + 4mM 4-NP; (c) Anodic and cathodic potentials (*E*<sub>pa/c</sub>) vs.  $\log \nu$ . recorded in 0.5M H<sub>2</sub>SO<sub>4</sub> with 4mM drug + 4mM 4-NP; (d) The plot of anodic peak current *I*<sub>pa</sub> in mA vs square root of scan rate in Vs<sup>-1</sup> for the M-MWCNT in 0.5M H<sub>2</sub>SO<sub>4</sub> with 4mM drug + 4mM 4-NP in the scan rate range from 10 to 100 mVs<sup>-1</sup>.

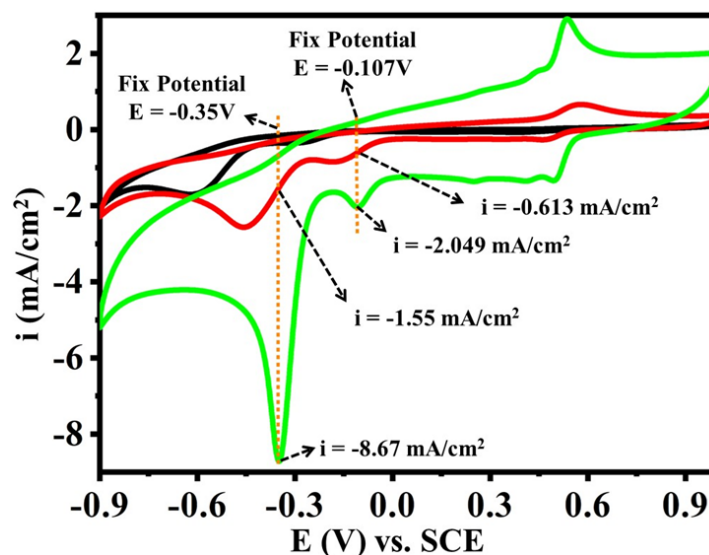


**Figure S6.** CV curves of Bare, CNT & CNT-Mel on 4mM drug + 4-NP at a scan rate of 50 mV/s

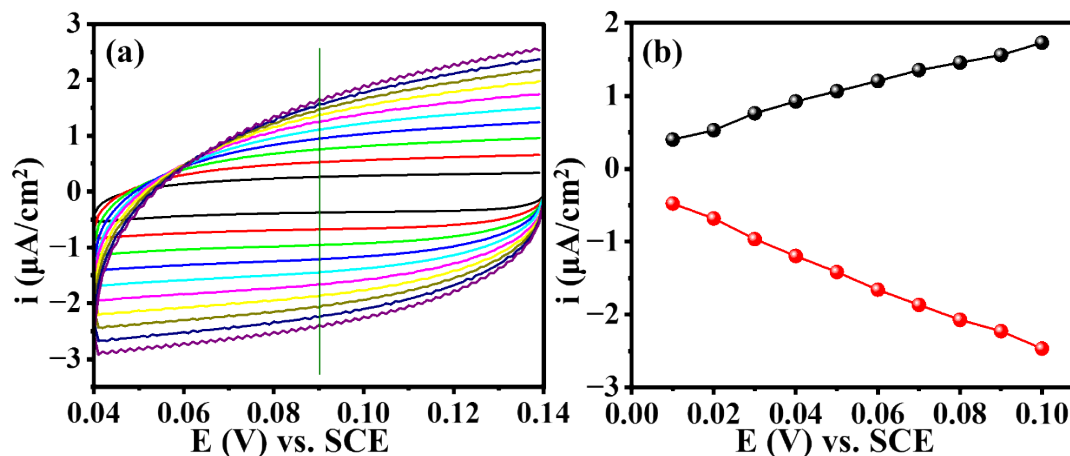


**Figure S7-**CV curves of the M-MWCNTs/GCE electrode in a non-Faradic area 4mM 4-NP and NFT in 0.5M H<sub>2</sub>SO<sub>4</sub> at the scan rates of 10, to 100 mV/s. (b) corresponding capacitive currents plotted as a function of the scan rate.

### Calculation for electrochemical active surface area:

Capacitive currents plotted as a function of the scan rate. *C*<sub>dl</sub> was calculated:

$$C_{dl} = (\text{Slope anodic} - \text{Slope cathodic})/2$$

ECSA was calculated over by the *C*<sub>dl</sub> using the specific surface capacitance (*C*<sub>s</sub>) of the electrode

surface:

$$ECSA = Cdl / C_s$$

Table S-1. Comparative electroanalytical parameters for the determination of NFT at M-MWC/GCE with previous reports.

| Sr. No. | Electrocatalyst                            | Methods    | Linear range ( $\mu\text{M}$ ) | LOD ( $\mu\text{M}$ ) | Reference        |
|---------|--|------------|--------------------------------|-----------------------|------------------|
| 1.      | AgSAE                                      | LSV        | 80.3–320.2                     | 47.9                  | [1]              |
| 2.      | CNF/SPCE                                   | DPV        | 0.2–100                        | 81                    | [2]              |
| 3.      | NSO/GCE                                    | i-t        | 0.006–466.67                   | 3                     | [3]              |
| 4.      | dsDNA/PAMT                                 | CV         | 6-100                          | 0.6                   | [4]              |
| 5.      | rGO/Fe <sub>3</sub> O <sub>4</sub> NRs/GCE | DPV        | 0.1–100                        | 0.083                 | [5]              |
| 6.      | AHD-McAb/GCE                               | CV         | 0.198–211.0                    | 0.198                 | [6]              |
| 7.      | <b>M-MWCNT</b>                             | <b>LSV</b> | <b>2-18</b>                    | <b>0.167</b>          | <b>This Work</b> |

Table S-2. Comparative electroanalytical parameters for the determination of 4-NP at M-MWC/GCE with previous reports.

| Sr. No. | Electrocatalyst                  | Methods     | Linear range ( $\mu\text{M}$ ) | LOD ( $\mu\text{M}$ ) | Reference        |
|---------|----------------------------------|-------------|--------------------------------|-----------------------|------------------|
| 1.      | Reduced graphene oxide (rGO)/GCE | DPV         | 50-800                         | 42                    | [7]              |
| 2.      | DTD/Ag NPs/GCE                   | CV          | 1-100                          | 0.25                  | [8]              |
| 3.      | rGO- Ag/GCE                      | Amperometry | 0.5-5.6                        | 0.32                  | [9]              |
| 4.      | FeOx/TiO <sub>2</sub> @mC/GCE    | Amperometry | 5-310                          | 0.183                 | [10]             |
| 5.      | CeO <sub>2</sub> -CuO/GCE        | CV          | 74-300                         | 2.03                  | [11]             |
| 6.      | CoOxNS/GCE                       | CV          | 20-240                         | 0.3                   | [12]             |
| 7.      | Zeolite/c-PANI-SSA/GCE           | CV          | 1-100                          | 1.27                  | [13]             |
| 8.      | <b>M-MWCNT</b>                   | <b>LSV</b>  | <b>2-18</b>                    | <b>0.165</b>          | <b>This Work</b> |

#### References:

[1] P. Salgado-Figueroa, P. Jara-Ulloa, A. Alvarez-Lueje, J.A. Squella, Sensitive determination of nitrofurantoin by flow injection analysis using carbon nanofiber screen printed electrodes, *Electroanalysis*. 25 (2013) 1433–1438. <https://doi.org/10.1002/elan.201300065>.

[2] Z. Krejčová, J. Barek, V. Vyskočil, Voltammetric determination of nitrofurantoin at a mercury meniscus modified silver solid amalgam electrode, *Electroanalysis*. 27 (2015) 185–192. <https://doi.org/10.1002/elan.201400410>.

[3] M. Annalakshmi, S. Sumithra, S.M. Chen, T.W. Chen, X.H. Zheng, Facile synthesis of ultrathin NiSnO<sub>3</sub> nanoparticles for enhanced electrochemical detection of an antibiotic drug in water bodies and biological samples, *New J. Chem.* 44 (2020) 10604–10612. <https://doi.org/10.1039/d0nj01375g>.

[4] G. Aydoğdu, G. Günendi, D.K. Zeybek, B. Zeybek, Ş. Pekyardımcı, A novel electrochemical DNA biosensor based on poly-(5-amino-2-mercapto-1, 3,4-thiadiazole) modified glassy carbon electrode for the determination of nitrofurantoin, *Sensors Actuators, B Chem.* 197 (2014) 211–219. <https://doi.org/10.1016/j.snb.2014.02.083>.

[5] B. He, J. Li, A sensitive electrochemical sensor based on reduced graphene oxide/Fe<sub>3</sub>O<sub>4</sub> nanorod composites for detection of nitrofurantoin and its metabolite, *Anal. Methods.* 11 (2019) 1427–1435. <https://doi.org/10.1039/c9ay00197b>.

[6] Q. Wang, Y.C. Liu, Y.J. Chen, W. Jiang, J.L. Shi, Y. Xiao, M. Zhang, Development of a direct competitive chemiluminescent ELISA for the detection of nitrofurantoin metabolite 1-amino-hydantoin in fish and honey, *Anal. Methods.* 6 (2014) 4414–4420. <https://doi.org/10.1039/c4ay00487f>.

[7] P. Wiench, B. Grzyb, Z. González, R. Menéndez, B. Handke, G. Gryglewicz, pH robust electrochemical detection of 4-nitrophenol on a reduced graphene oxide modified glassy carbon electrode, *J. Electroanal. Chem.* 787 (2017) 80–87. <https://doi.org/10.1016/j.jelechem.2017.01.040>.

[8] G. Rounaghi, R.M. Kakhki, H. Azizi-Toupkanloo, Voltammetric determination of 4-nitrophenol using a modified carbon paste electrode based on a new synthetic crown ether/silver nanoparticles, *Mater. Sci. Eng. C.* 32 (2012) 172–177. <https://doi.org/10.1016/j.msec.2011.10.014>.

[9] Y. Tang, R. Huang, C. Liu, S. Yang, Z. Lu, S. Luo, Electrochemical detection of 4-nitrophenol based on a glassy carbon electrode modified with a reduced graphene oxide/Au nanoparticle composite, *Anal. Methods.* 5 (2013) 5508–5514. <https://doi.org/10.1039/c3ay40742j>.

[10] M. Wang, Y. Liu, L. Yang, K. Tian, L. He, Z. Zhang, Q. Jia, Y. Song, S. Fang, Bimetallic metal–organic framework derived FeOx/TiO<sub>2</sub> embedded in mesoporous carbon nanocomposite for the sensitive electrochemical detection of 4-nitrophenol, *Sensors Actuators, B Chem.* 281 (2019) 1063–1072. <https://doi.org/10.1016/j.snb.2018.11.083>.

- [11] S.B. Khan, K. Akhtar, E.M. Bakhsh, A.M. Asiri, Electrochemical detection and catalytic removal of 4-nitrophenol using CeO<sub>2</sub>-Cu<sub>2</sub>O and CeO<sub>2</sub>-Cu<sub>2</sub>O/CH nanocomposites, *Appl. Surf. Sci.* 492 (2019) 726–735. <https://doi.org/10.1016/j.apsusc.2019.06.205>.
- [12] A. Noorbakhsh, M.M. Mirkaei, M.H. Yousefi, S. Manochehri, Electrodeposition of cobalt oxide nanostructure on the glassy carbon electrode for electrocatalytic determination of para-Nitrophenol, *Electroanalysis*. 26 (2014) 2716–2726. <https://doi.org/10.1002/elan.201400386>.
- [13] A. Jović, A. Đorđević, M. Čebela, I. Stojković Simatović, R. Hercigonja, B. Šljukić, Composite zeolite/carbonized polyaniline electrodes for p-nitrophenol sensing, *J. Electroanal. Chem.* 778 (2016) 137–147. <https://doi.org/10.1016/j.jelechem.2016.08.025>.